Check for updates

Advanced Physics Research

ADVANCED PHYSICS RESEARCH Open Access

www.advphysicsres.com

RESEARCH ARTICLE OPEN ACCESS

Resonant Tunneling in Laser-Dressed Double-Barrier Nanostructures: Role of Potential Geometry

Recep Aydın[1] | Mehmet Batı[2]

[1]Department of Electrical and Electronic Engineering, Recep Tayyip Erdoğan University, Rize, Türkiye | [2]Department of Physics, Recep Tayyip Erdoğan University, Rize, Türkiye

Correspondence: Recep Aydın (recep_aydin24@erdogan.edu.tr) | Mehmet Batı (mehmet.bati@erdogan.edu.tr)

Received: 26 January 2026 | **Revised:** 21 May 2026 | **Accepted:** 29 May 2026

Keywords: double-barrier nanostructures | external electric field | laser-dressed potential | quantum confinement | resonant tunneling | semiconductor nanostructures | transfer matrix method

ABSTRACT

This work examines resonant tunneling in laser-dressed double-barrier semiconductor nanostructures using the transfer matrix method. Rectangular, parabolic, and triangular barrier geometries are considered to examine the influence of potential shape on resonance tunneling behavior. The effect of an intense laser field is treated within the effective mass and high-frequency approximation, with the roles of the external electric field, barrier height, and well width. The results show that increasing the laser field parameter significantly lowers the resonance energies due to laser-induced modification of the effective confinement potential. External electric fields produce Stark-like shifts. Barrier height variations lead to a shift of resonance energies to higher energy, reflecting stronger confinement, while increasing the well width causes a pronounced reduction in resonance energies as a consequence of weakened quantum confinement. Among the investigated geometries, parabolic barriers display smoother and more stable resonance evolution, whereas triangular barriers show stronger tunability under external perturbations. These findings demonstrate that the combined use of laser dressing and potential shape engineering provides an efficient mechanism for controlling resonant tunneling characteristics in nanoscale electronic and optoelectronic devices.

1 | Introduction

Resonant tunneling in double-barrier nanostructures is a fundamental problem in low-dimensional quantum transport, with direct relevance to nanoscale electronic and optoelectronic devices. Conventionally, such systems are modeled using rectangular double-barrier potentials, which provide a clear framework for understanding quantum interference, quasi-bound states, and energy-selective transmission [1–5]. Precise control of barrier parameters such as potential height, width, and shape is essential for tailoring resonant conditions and optimizing carrier transport properties.

A variety of theoretical and numerical techniques have been developed to analyze resonant tunneling phenomena [8–12]. Among these approaches, the non-equilibrium Green's function (NEGF) approach and transfer matrix method (TMM) are particularly well suited for investigations focusing on transmission properties and resonance tunneling conditions. The TMM has emerged as a robust and efficient approach for calculating transmission coefficients and resonant energy levels in layered quantum systems [1–8]. Owing to its numerical stability and flexibility, TMM allows accurate modeling of wave-function continuity across heterointerfaces and can be readily adapted to different potential profiles.

[Correction added on June 24, 2026, after first online publication: email ID for first author has been update in this version.]

This is an open access article under the terms of the Creative Commons Attribution License, which permits use, distribution and reproduction in any medium, provided the original work is properly cited.

© 2026 The Author(s). *Advanced Physics Research* published by Wiley-VCH GmbH

Beyond conventional rectangular barriers, advances in nanofabrication have enabled the realization of quantum structures with non-rectangular geometries, including parabolic and triangular barrier profiles. These alternative geometries introduce additional degrees of freedom for engineering quantum confinement and interference effects. Previous studies have shown that barrier shape can significantly influence the position, width, and amplitude of resonance peaks, highlighting the importance of comparative analyses across different potential profiles [12–15].

In addition to structural design, external fields provide a powerful means of dynamically tuning resonant tunneling behavior. In particular, intense laser fields can effectively modify the confinement potential experienced by charge carriers, giving rise to laser-dressed potentials. Such laser-induced modifications can shift resonant energy levels, alter transmission probabilities, and reorganize electronic states without changing the physical geometry of the structure. As a result, intense laser fields serve as an external control parameter for quantum transport [16–25]. Recent studies have highlighted the increasing importance of external field-assisted quantum transport and geometry-dependent confinement effects in semiconductor nanostructures [20–25]. In particular, laser-assisted resonance tunneling has been shown to provide an effective mechanism for modifying electronic structure and transport properties via laser-dressed potentials [21–24]. At the same time, advances in numerical modeling and device-oriented simulations have emphasized the critical role of structural parameters and potential geometry in determining resonant states and transport characteristics [21–24].

Despite these advances, systematic comparative analysis of different barrier geometries under intense laser fields remains limited. Although intense laser field effects have been extensively investigated in various quantum well systems, often in the context of optical and nonlinear response properties [25–30], their influence on resonant tunneling through double-barrier structures with different barrier geometries remains comparatively underexplored. In particular, systematic studies comparing rectangular, parabolic, and triangular double-barrier profiles under intense laser fields are limited. Moreover, the present study reveals distinct geometry-dependent physical mechanisms governing the laser-induced evolution of resonant states. In parabolic double-barrier structures, the smooth spatial variation of the confinement potential suppresses abrupt scattering effects and leads to more stable and regular resonance shifts under laser-field modulation. In contrast, triangular barriers exhibit enhanced sensitivity to external perturbations due to their intrinsic asymmetry, which amplifies laser-induced distortion of the effective confinement landscape and promotes stronger wavefunction redistribution. These contrasting behaviors provide new physical understanding into how barrier geometry controls the stability and tunability of resonant tunneling states under intense laser dressing, an aspect that has not been systematically clarified in previous comparative studies.

Motivated by this deficiency, we investigate resonant tunneling properties in double-barrier quantum structures with rectangular, parabolic, and triangular barrier geometries under intense laser fields. Using the transfer matrix method, we focus on laser-induced modifications of resonant tunneling energy. For the purpose of designing and optimizing tunable quantum electronic systems, the results enable a clear comparison of how barrier geometry and external laser fields together control tunneling behavior.

Unlike most previous studies that primarily investigate resonant tunneling behavior for a single potential geometry or focus on current-voltage characteristics using non-equilibrium Green's function approaches, the present work provides a systematic comparative analysis of rectangular, parabolic, and triangular double-barrier structures within a unified laser-dressed transport framework. This comparative treatment enables a transparent identification of geometry-dependent resonance tunability mechanisms under intense laser-field conditions and reveals how confinement reshaping depends on barrier profile selection. Such a unified geometry-dependent analysis under laser-field modulation remains limited in the existing literature.

2 | Model and Theory

2.1 | Physical Model and Laser-Dressed Potential

We consider a one-dimensional double-barrier nanostructure composed of two finite potential barriers separated by a quantum well. The system is modeled within the effective mass approximation, assuming coherent and elastic electron transport along the growth direction. The spatial geometry consists of a left barrier of width L_B, a quantum well of width L_W, and a right barrier of width R_B. Outside the active region, the potential is assumed to be zero, corresponding to free-electron propagation in the leads. In the absence of external fields, the confinement potential is defined by the barrier heights V_L and V_R, which may assume different spatial profiles depending on the barrier geometry. In this work, three representative barrier shapes are investigated: rectangular, parabolic, and triangular profiles. These geometries allow a systematic comparison of how barrier shape influences resonant tunneling behavior.

To account for the influence of an intense laser field, the system is described using a laser-dressed potential formalism. Within the high-frequency and dipole approximations, the effect of the intense laser field can be incorporated as an effective modification of the confinement potential, leading to a renormalized, field-dependent potential landscape. The strength of the laser field is characterized by the dimensionless laser parameter α_0, which is proportional to the ratio of the laser-induced oscillation amplitude to the effective Bohr radius. As a result, the effective potential becomes explicitly dependent on the laser field intensity, allowing dynamic control of resonance conditions without altering the physical geometry of the structure. Figure 1 shows the spatial profiles of the double-barrier potentials for (a) rectangular, (b) parabolic, and (c) triangular barrier geometries under different laser field conditions. The black solid curves represent the field-free potential, while the blue and red dashed curves correspond to increasing values of the laser field parameter ($\alpha_0 = 3$ and 5 nm). In the absence of the laser field, all three structures exhibit well-defined double-barrier profiles with a confined quantum well region at the center. When the intense laser field is applied, the effective potential undergoes a pronounced modification, commonly referred to as laser dressing. This effect leads to a reduction of the effective barrier height and a softening of the confinement potential inside the quantum well.

27511200, 2026, 8, Downloaded from https://advanced.onlinelibrary.wiley.com/doi/10.1002/apxr.70152 by Recep Tayyip Erdoan Universitesi, Wiley Online Library on [24/11/2026]. See the Terms and Conditions (https://onlinelibrary.wiley.com/terms-and-conditions) on Wiley Online Library for rules of use; OA articles are governed by the applicable Creative Commons License

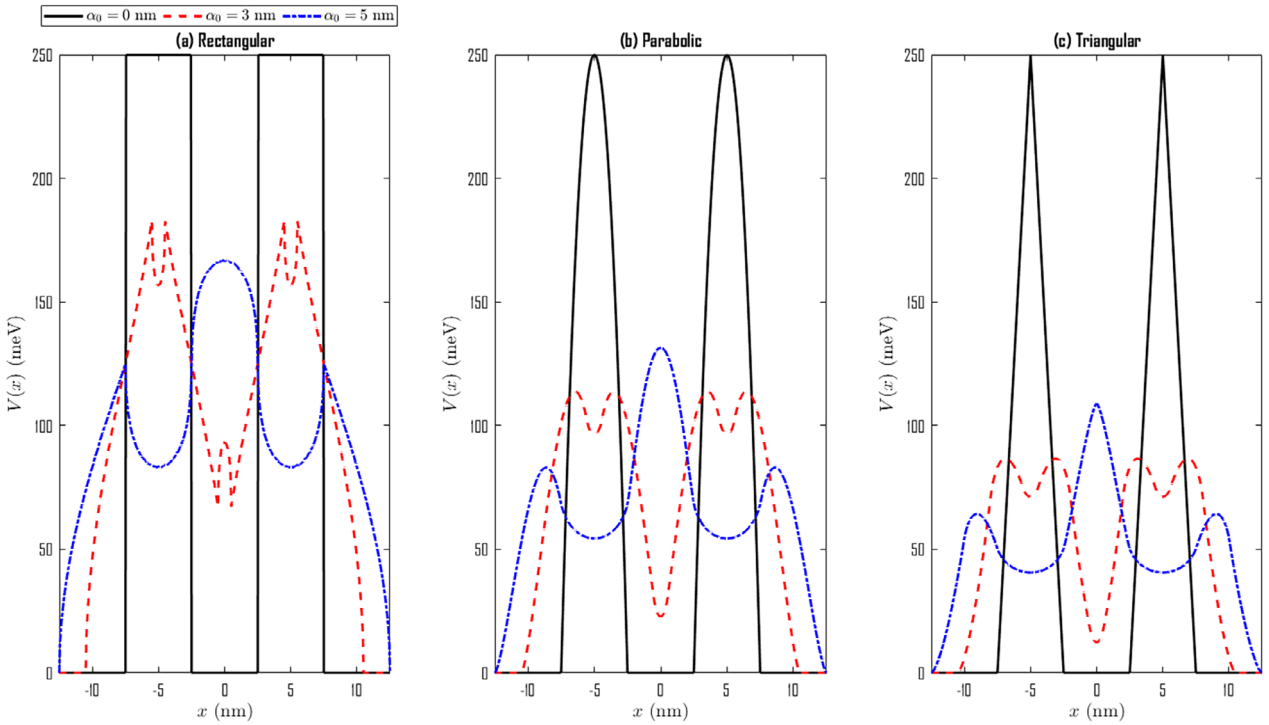

FIGURE 1 | Spatial profiles of double-barrier potentials for (a) rectangular, (b) parabolic, and (c) triangular geometries under different laser field conditions. The black solid curves denote the field-free potentials, while the red ($\alpha_0 = 3$ nm) and blue ($\alpha_0 = 5$ nm) dashed curves represent the laser-dressed effective potentials. The intense laser field progressively softens the confinement potential, reduces the effective barrier height, and reshapes the quantum well in a geometry-dependent manner. As a result, enhanced wave-function penetration into the barrier regions and laser-induced shifts of the resonance energies are observed.

All spatial coordinates and energies are expressed in dimensionless units by scaling lengths with the effective Bohr radius a_0^* and energies with the effective Hartree energy E_H^*. This scaling simplifies the numerical implementation.

2.2 | Schrödinger Equation and Transfer Matrix Formalism

The stationary electron states are governed by the one-dimensional time-independent Schrödinger equation

$$-\frac{\hbar^2}{2m^*}\frac{d^2\psi}{dx^2} + V_{eff}(x,\alpha_0)\psi = E\psi \tag{1}$$

where $V_{eff}(x,\alpha_0)$ denotes the laser-dressed confinement potential and E is the electron energy. The structure is discretized into sufficiently small spatial segments such that the potential within each segment can be considered locally constant. In each segment n, the wave function can be written as a superposition of forward- and backward-propagating plane waves,

$$\psi_n = A_n\, e^{ik_n x} + B_n e^{-ik_n x} \tag{2}$$

with the local wave vector given by $k_n = \sqrt{2[E - V_{eff}(x_n)]}$.

At each interface between adjacent segments, continuity of the wave function and its derivative is enforced. These boundary conditions relate the wave amplitudes in neighboring regions through an interface matrix, while free propagation within each segment is described by a propagation matrix. The total transfer matrix M of the system is obtained by sequentially multiplying the interface and propagation matrices across the entire structure [30].

Within the effective mass approximation, electron transport is assumed to remain coherent and elastic across the structure. The laser-field interaction is incorporated through a high-frequency Floquet-type dressing approach, which results in an effective static potential modification depending on the laser parameter α_0. This approximation is well established for describing intense non-resonant laser-field effects in semiconductor heterostructures and allows the treatment of laser-induced confinement reshaping within a stationary transport framework.

2.3 | Transmission Coefficient

Once the total transfer matrix M is constructed, the transmission coefficient is calculated from the matrix element M_{11}. For an electron incident from the left lead with wave vector k_{in} and transmitted to the right lead with wave vector k_{out}, the transmission probability is given by

$$T(E) = Re\left(\frac{k_{out}}{k_{in}}\right)\frac{1}{|M_{11}^2|} \tag{3}$$

This expression ensures current conservation and remains valid for both symmetric and asymmetric barrier configurations. Since

27511200, 2026, 8, Downloaded from https://advanced.onlinelibrary.wiley.com/doi/10.1002/apxr.70152 by Recep Tayyip Erdoan Universitesi, Wiley Online Library on [24/11/2026]. See the Terms and Conditions (https://onlinelibrary.wiley.com/terms-and-conditions) on Wiley Online Library for rules of use; OA articles are governed by the applicable Creative Commons License

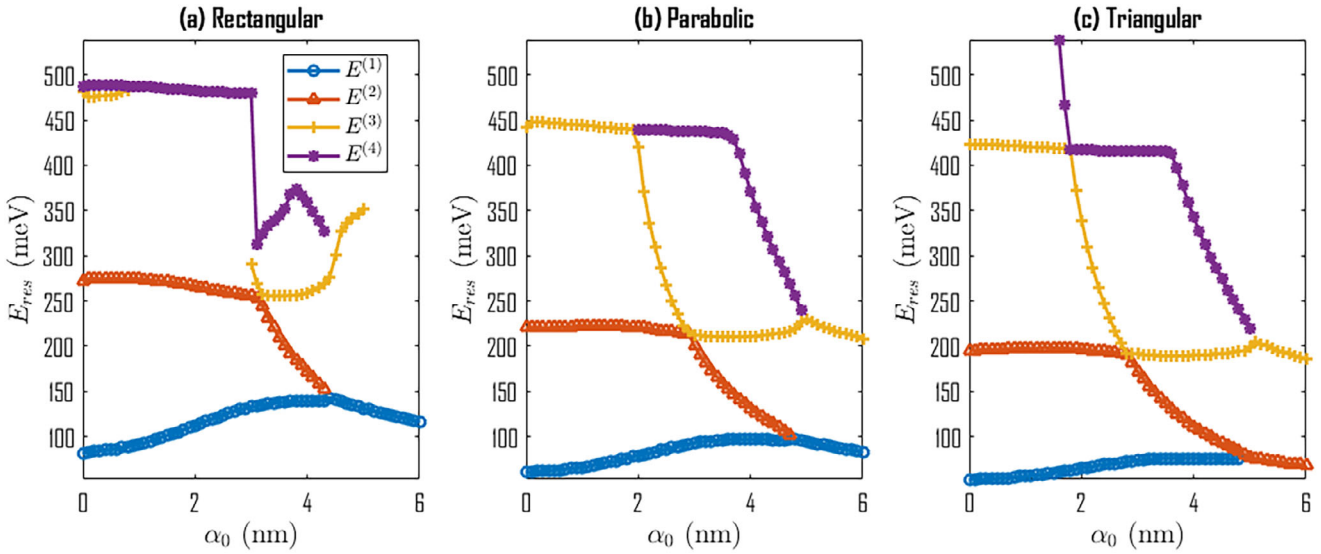

FIGURE 2 | Variation of the resonance energies $E_{res}^{(n)}$ as a function of the laser field parameter α_0 for (a) rectangular, (b) parabolic, and (c) triangular double-barrier structures. The barrier heights are fixed at 250 meV, with barrier and well widths set to 5 nm, and the external electric field is set to $F = 0$ kV/cm. Increasing α_0 leads to pronounced, geometry-dependent shifts of the resonance energies, reflecting the laser-induced softening of the confinement potential and the modification of the effective quantum well depth.

the present study focuses on zero-bias conditions, the transmission coefficient fully characterizes the resonant tunneling behavior of the system.

For the numerical calculations, the spatial domain is discretized using a uniform grid with a sufficiently small step size to accurately resolve rapid variations in the wave function near the barrier interfaces. The laser-dressed potential is evaluated on this grid for each barrier geometry and laser field strength. The transmission coefficient is computed over a dense energy grid covering the relevant energy range. Resonant states are identified as pronounced peaks in the transmission spectrum. Parallel computation is employed to accelerate the energy-resolved transmission calculations, as each energy point can be treated independently. This approach significantly reduces computation time while preserving numerical accuracy.

The transfer matrix method used in the present study has been widely validated for coherent quantum transport problems in layered semiconductor nanostructures and provides results consistent with alternative approaches such as non-equilibrium Green's function and Schrödinger-Poisson simulations for transmission spectra and resonance energies [10, 21]. Since the focus of the present work is on geometry-dependent resonance evolution under laser-field modulation rather than current–voltage characteristics, the transfer matrix framework represents a computationally efficient and physically transparent approach.

3 | Results and Discussion

3.1 | Effect of the Intense Laser Field on Resonance Energies

Figure 2 illustrates the variation of the first four resonance energies $E_{res}^{(n)}$ as a function of the intense laser field parameter α_0 for double-barrier quantum structures with (a) rectangular, (b) parabolic, and (c) triangular double barrier profiles. Unless otherwise stated, the barrier heights are fixed at 250 meV, the well and barrier widths are set to 5 nm, and the external electric field is taken as $F = 0$ kV/cm.

For all barrier geometries, the resonance energies exhibit a pronounced dependence on the laser field parameter, demonstrating that the intense laser field acts as an effective external control knob for tuning the electronic states. However, the magnitude and qualitative behavior of these shifts strongly depend on the barrier geometry.

In the case of the rectangular barrier (Figure 2a), the lowest resonance energy $E_{res}^{(1)}$ shows a gradual increase with increasing α_0 up to intermediate laser field strengths, followed by a slight saturation at higher values. Higher-order resonances display more complex behavior, including non-monotonic variations and abrupt changes in slope around specific laser field values. This behavior can be attributed to laser-induced restructuring of quasi-bound states inside the quantum well, which arises from the modification of the effective confinement potential under strong laser dressing. For the parabolic barrier geometry (Figure 2b), the resonance energies exhibit significantly stronger sensitivity to the laser field. In particular, the higher-order resonances undergo rapid shifts toward lower energies beyond a critical value of α_0. This enhanced tunability can be attributed to the smooth curvature of the parabolic potential, which allows the intense laser field to more efficiently reshape the confinement profile and redistribute the electronic probability density. As a result, level repulsion and crossing-like behaviors become more pronounced compared to the rectangular case. The triangular barrier structure (Figure 2c) presents an intermediate but distinctly asymmetric response to the laser field. While the lowest resonance energy increases slowly with α_0, higher resonances exhibit steep energy shifts and, in some cases, sudden drops as the laser field strength

27511200, 2026, 8, Downloaded from https://advanced.onlinelibrary.wiley.com/doi/10.1002/apxr.70152 by Recep Tayyip Erdoan Üniversitesi, Wiley Online Library on [24/11/2026]. See the Terms and Conditions (https://onlinelibrary.wiley.com/terms-and-conditions) on Wiley Online Library for rules of use; OA articles are governed by the applicable Creative Commons License

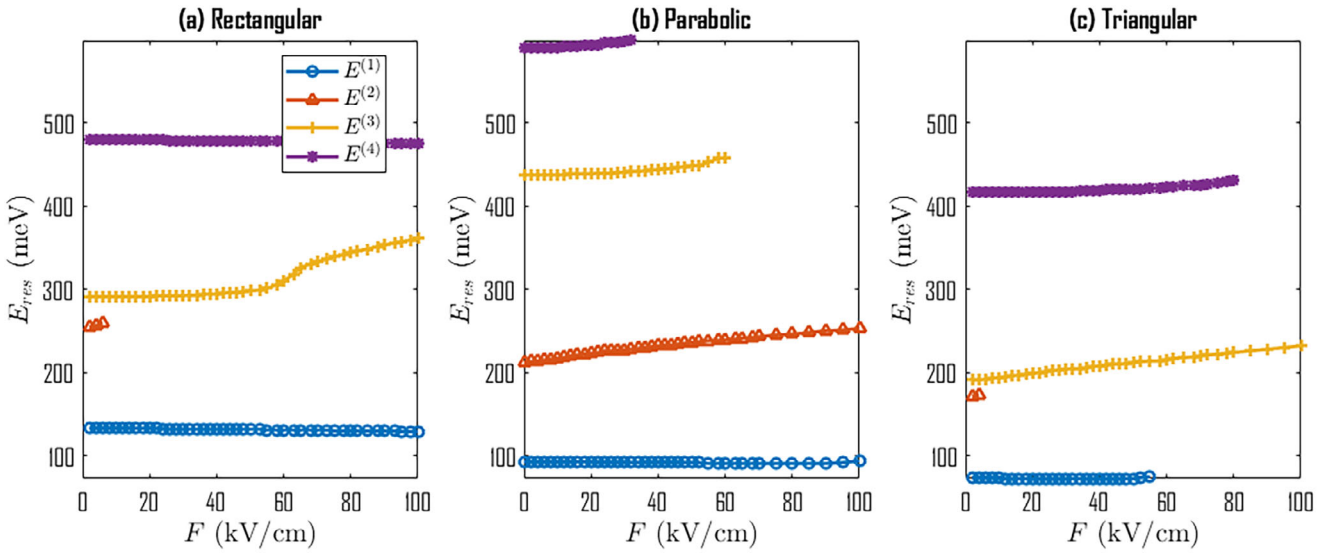

FIGURE 3 | Dependence of the resonance energies $E_{res}^{(n)}$ on the external electric field F for (a) rectangular, (b) parabolic, and (c) triangular double-barrier geometries at a fixed laser field parameter $\alpha_0 = 3$ nm. The applied electric field tilts the confinement potential, resulting in Stark-like shifts of the resonance levels. The magnitude and monotonicity of these shifts depend strongly on the barrier geometry, with higher-energy resonant states exhibiting enhanced sensitivity to the external field.

increases. This behavior reflects the inherent asymmetry of the triangular potential, which leads to an uneven laser-induced distortion of the effective potential landscape and consequently affects the spatial localization of the resonant states.

3.2 | Effect of the External Electric Field on Resonance Energies

Figure 3 presents the dependence of the first four resonance energies on the external electric field F for double-barrier structures with rectangular, parabolic, and triangular barrier profiles. In these calculations, the barrier heights are fixed at 250 meV, the well and barrier widths are 5 nm, and the intense laser field parameter is set to $\alpha_0 = 3$ nm.

For all barrier geometries, the application of an external electric field results in systematic shifts of the resonance energies, reflecting the field-induced tilting of the effective confinement potential. The lowest resonance energy exhibits a relatively weak dependence on the electric field, whereas higher-order resonances display more pronounced shifts as F increases.

In the rectangular barrier case (Figure 3a), the resonance energies remain nearly constant at low electric field strengths and begin to vary more noticeably only at higher fields. This behavior indicates that the symmetric and abrupt nature of the rectangular barriers provides strong confinement, making the system relatively robust against moderate electric field perturbations. The observed shifts at higher fields can be attributed to the Stark effect, which modifies the spatial localization of the quasi-bound states inside the quantum well. For the parabolic barrier geometry (Figure 3b), the resonance energies increase almost linearly with the applied electric field. The smoother confinement profile enhances the sensitivity of the electronic states to the external field, leading to stronger Stark shifts compared to the rectangular case. This linear trend suggests that parabolic barriers allow more efficient field-induced redistribution of the wave function across the well-barrier regions. The triangular barrier structure (Figure 3c) exhibits an intermediate response, with resonance energies showing gradual and nearly linear increases with the electric field. Due to the intrinsic asymmetry of the triangular potential, the applied field further enhances the asymmetry of the confinement, resulting in geometry-dependent energy shifts. These results demonstrate that barrier shape plays a crucial role in determining the strength of electric-field-induced tuning of resonance energies.

3.3 | Effect of Barrier Height on Resonance Energies

The effect of barrier height V_B on the resonance energies is shown in Figure 4 for rectangular, parabolic, and triangular double-barrier structures. The calculations are performed under zero external electric field and fixed laser field conditions $\alpha_0 = 3$ nm.

As expected, increasing the barrier height leads to a systematic increase in all resonance energies for all geometries. This behavior arises from the enhanced confinement of electrons within the quantum well, which raises the energy of the quasi-bound states. The lowest resonance energy increases almost linearly with V_B, while higher-order resonances exhibit steeper slopes, indicating stronger sensitivity to barrier height variations. In the rectangular barrier configuration (Figure 4a), the resonance energies show clear linear trends with increasing V_B reflecting the strong and well-defined confinement provided by the abrupt barrier interfaces. The higher resonances display slightly nonlinear behavior at large barrier heights, which can be attributed to changes in tunneling probability and wave-function penetration depth. For the parabolic barrier (Figure 4b), the resonance energies increase

27511200, 2026, 8, Downloaded from https://advanced.onlinelibrary.wiley.com/doi/10.1002/apxr.70152 by Recep Tayyip Erdoan Üniversitesi, Wiley Online Library on [24/11/2026]. See the Terms and Conditions (https://onlinelibrary.wiley.com/terms-and-conditions) on Wiley Online Library for rules of use; OA articles are governed by the applicable Creative Commons License

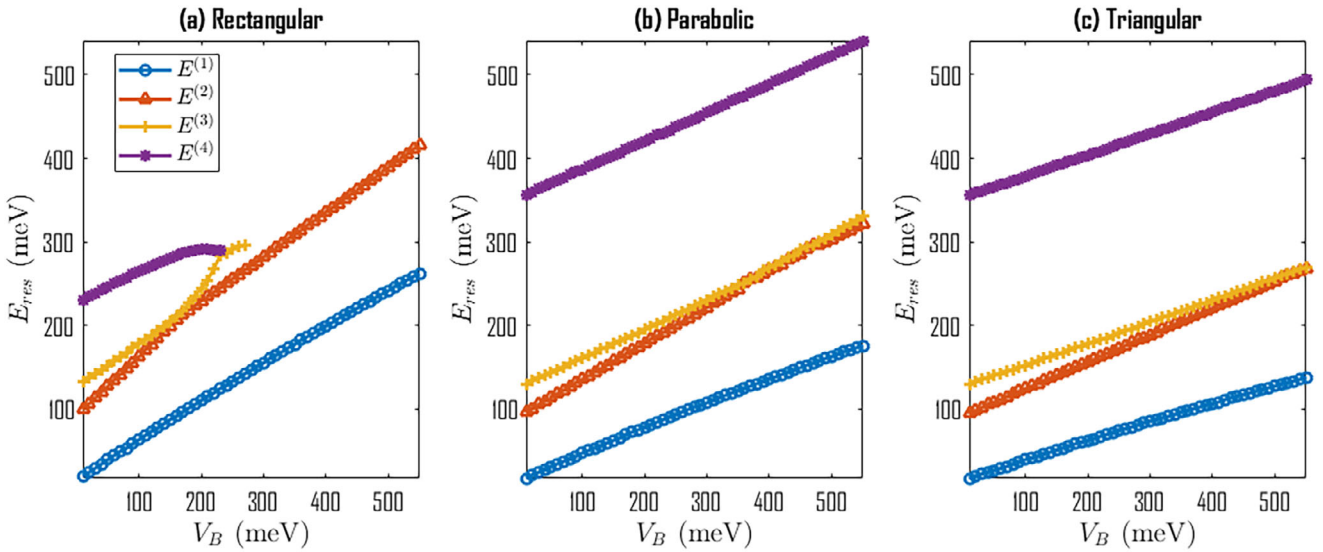

FIGURE 4 | Resonance energies $E_{res}^{(n)}$ as a function of the barrier height V_B for (a) rectangular, (b) parabolic, and (c) triangular double-barrier structures at fixed well and barrier widths of 5 nm. Increasing V_B systematically raises the resonance energies due to stronger quantum confinement. The nearly linear dependence observed for parabolic and triangular barriers highlights the role of potential geometry in determining the confinement strength and the spacing between resonant states.

more uniformly and with nearly constant slopes across the entire barrier height range. This indicates that parabolic confinement leads to smoother energy scaling and reduced sensitivity to abrupt changes in the potential profile. As a result, parabolic barriers offer predictable and controllable tuning of resonance energies through barrier height engineering. The triangular barrier geometry (Figure 4c) again exhibits intermediate behavior. While resonance energies increase monotonically with barrier height, the slopes differ from those of the rectangular and parabolic cases. The asymmetric nature of the triangular potential leads to uneven confinement, which affects higher-order resonances more strongly than the ground state.

3.4 | Effect of Well Width on Resonance Energies

Figure 5 illustrates the variation of the first four resonance energies as a function of the well width L_W for rectangular, parabolic, and triangular double-barrier structures. All other parameters are kept fixed in order to isolate the influence of the quantum well width on the resonant states.

For all barrier geometries, an increase in the well width leads to a pronounced decrease in the resonance energies. This behavior is a direct consequence of quantum confinement: as the well becomes wider, the spatial confinement of the electron is reduced, resulting in lower energy eigenstates. The effect is strongest for the lowest resonance and gradually weakens for higher-order resonances. In the rectangular barrier case (Figure 5a), the resonance energies decrease rapidly with increasing L_W , particularly for small well widths. At larger L_W. , the energy levels approach asymptotic values, indicating the gradual transition toward quasi-continuum behavior inside the well. The higher resonances exhibit non-monotonic features and level repulsion in certain width ranges, which can be attributed to enhanced coupling between quasi-bound states and tunneling channels through the barriers. For the parabolic barrier geometry (Figure 5b), the resonance energies show smoother and more monotonic decreases with increasing well width. The absence of abrupt interfaces reduces scattering effects and suppresses strong level interactions, leading to more regular energy spacing. This behior highlights the stabilizing role of parabolic confinement on resonant states, particularly for higher energy levels. In the triangular barrier structure (Figure 5c), the resonance energies decrease sharply at small well widths and then gradually level off as L_W increases. Due to the intrinsic asymmetry of the triangular potential, higher resonances are more sensitive to changes in well width, resulting in stronger shifts compared to the rectangular and parabolic cases. The asymmetry enhances wave-function leakage toward one side of the structure, modifying the effective confinement length.

The geometry-dependent tunability of resonance energies demonstrates that double-barrier structures can be effectively engineered through appropriate selection of barrier profiles and external field conditions. In particular, the enhanced sensitivity of parabolic and triangular geometries highlights the strong influence of potential shape on resonant tunneling behavior. Furthermore, intense laser fields provide an additional degree of control by non-invasively modifying the effective confinement potential.

4 | Conclusion

In this work, the resonant tunneling characteristics of double-barrier nanostructures under intense laser fields have been analyzed for rectangular, parabolic, and triangular double barrier geometries within the framework of the transfer matrix method. The study provides a comprehensive comparison of how laser dressing and structural parameters collectively influence the resonance spectrum.

27511200, 2026, 8, Downloaded from https://advanced.onlinelibrary.wiley.com/doi/10.1002/apxr.70152 by Recep Tayyip Erdoan Üniversitesi, Wiley Online Library on [24/11/2026]. See the Terms and Conditions (https://onlinelibrary.wiley.com/terms-and-conditions) on Wiley Online Library for rules of use; OA articles are governed by the applicable Creative Commons License

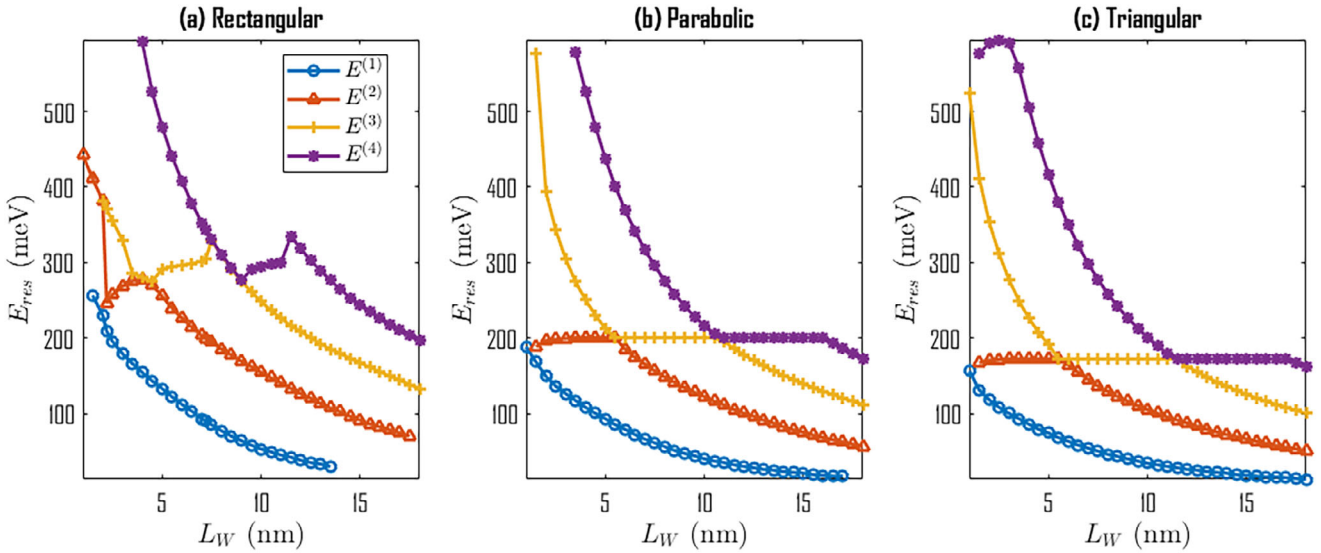

FIGURE 5 | Variation of the resonance energies $E_{res}^{(n)}$ with the quantum well width L_W for different barrier geometries. An increase in L_W results in a downward shift of the resonance energies, consistent with reduced quantum confinement. Higher-order resonant states exhibit stronger sensitivity to well-width variations, emphasizing the importance of geometric tuning in double-barrier nanostructures.

The results show that the laser field effectively reshapes the confinement potential, leading to a systematic reduction of resonance energies as the laser parameter increases. The influence of an external electric field further introduces Stark-like shifts, with asymmetric barrier profiles exhibiting stronger energy modulation. Barrier height variations lead to a monotonic increase in resonance energies, confirming that stronger barriers enhance confinement and raise quasi-bound state energies. In contrast, increasing the well width significantly lowers resonance energies for all geometries, consistent with fundamental quantum confinement principles. Among the considered structures, parabolic barriers provide the smoothest and most regular resonance evolution, while triangular barriers exhibit enhanced sensitivity to both laser and electric fields.

The present results demonstrate that resonance energies in double-barrier systems can be efficiently tuned through a combination of laser field control. These findings demonstrate that the combined use of laser-field control and potential-shape engineering provides a powerful and flexible strategy for tailoring resonance spectra in semiconductor nanostructures, offering promising opportunities for the development of tunable quantum transport devices and next-generation optoelectronic applications.

Funding

The authors have nothing to report.

Conflicts of Interest

The authors declare no conflicts of interest.

Data Availability Statement

The data that support the findings of this study are available from the corresponding author upon reasonable request.

References

1. L. Esaki, "New Phenomenon in Narrow Germanium p−n Junctions," *Physical Review* 109 (1958): 603–604, https://doi.org/10.1103/physrev.109.603.

2. D. K. Ferry, S. M. Goodnick, and J. Bird, *Transport in Nanostructures* (Cambridge University Press, 2009), https://doi.org/10.1017/CBO9780511840463.

3. L. Esaki, "Long Journey Into Tunneling," *Science* 183 (1974): 1149–1155, https://doi.org/10.1126/science.183.4130.1149.

4. L. Esaki and R. Tsu, "Superlattice and Negative Differential Conductivity in Semiconductors," *IBM Journal of Research and Development* 14 (1970): 61–65, https://doi.org/10.1147/rd.141.0061.

5. L. L. Chang, L. Esaki, and R. Tsu, "Resonant Tunneling in Semiconductor Double Barriers," *Applied Physics Letters* 24 (1974): 593–595, https://doi.org/10.1063/1.1655067.

6. F. Nutku, "Quasi-Bound Levels, Transmission and Resonant Tunneling in Heterostructures with Double and Multi Rectangular, Trapezoidal, Triangular Barriers," *Journal of Computational Electronics* 13 (2014): 456–465, https://doi.org/10.1007/s10825-014-0556-1.

7. J. Figueroa, I. Gonzalez, and D. Salinas-Arizmendi, "A Novel Transfer Matrix Framework for Multiple Dirac Delta Potentials," *Physics Letters A* 555 (2025): 130785, https://doi.org/10.1016/j.physleta.2025.130785.

8. D. K. Ferry, "An Introduction to Quantum Transport in Semiconductors," in *Pan Stanford eBooks* (2017), https://doi.org/10.1201/9781315206226.

9. L. R. N. Oliveira and M. G. E. Da Luz, "Quantum Scattering in One-Dimensional Periodic Structures: A Green's Function Approach Solved Through Continued Fractions," *Physical Review B* 110 (2024): 054303, https://doi.org/10.1103/PhysRevB.110.054303.

10. S. Datta, *Quantum Transport: Atom to transistor* (Cambridge University Press eBooks, 2005), https://doi.org/10.1017/cbo9781139164313.

11. V. N. Do, P. Dollfus, and V. L. Nguyen, "Transport and Noise in Resonant Tunneling Diode Using Self-Consistent Green's Function Calculation," *Journal of Applied Physics* 100 (2006): 093705, https://doi.org/10.1063/1.2364035.

12. M. Ohmukai, "Triangular Double Barrier Resonant Tunneling," *Materials Science and Engineering: B* 116 (2004): 87–90, https://doi.org/10.1016/j.mseb.2004.09.021.

27511200, 2026, 8, Downloaded from https://advanced.onlinelibrary.wiley.com/doi/10.1002/apxr.70152 by Recep Tayyip Erdoan Universitesi, Wiley Online Library on [24/11/2026]. See the Terms and Conditions (https://onlinelibrary.wiley.com/terms-and-conditions) on Wiley Online Library for rules of use; OA articles are governed by the applicable Creative Commons License

13. M. Bati, "The Effects of the Intense Laser Field on the Resonant Tunneling Properties of the Symmetric Triple Inverse Parabolic Barrier Double Well Structure," *Physica B: Condensed Matter* 594 (2020): 412314, https://doi.org/10.1016/j.physb.2020.412314.

14. M. Bati, S. Sakiroglu, and I. Sokmen, "Electron Transport in Electrically Biased Inverse Parabolic Double-Barrier Structure," *Chinese Physics B* 25, no. 5 (2016): 057307, https://doi.org/10.1088/1674-1056/25/5/057307.

15. A. Ukan, A. Hatipoğlu, and M. Batı, "Resonant Tunneling Properties of Inverse Parabolic Multibarrier Structures: A Non-Equilibrium Green's Function Approach," *Applied Physics A* 132, no. 1 (2025): 9, https://doi.org/10.1007/s00339-025-09194-3.

16. J. Kamiński and E. Saczuk, "Resonant Tunneling Controlled by Laser and Constant Electric Fields," *Acta Physica Polonica A* 122, no. 1 (2012): 53–62, https://doi.org/10.12693/aphyspola.122.53.

17. H. S. Brandi, A. Latgé, and L. E. Oliveira, "Dressed-Band Approach to Laser-Field Effects in Semiconductors and Quantum-Confined Heterostructures," *Physical Review B* 64, no. 3 (2001): 035323, https://doi.org/10.1103/physrevb.64.035323.

18. S. Aktas, H. Kes, F. Boz, and S. Okan, "Control of a Resonant Tunneling Structure by Intense Laser Fields," *Superlattices and Microstructures* 98 (2016): 220–227, https://doi.org/10.1016/j.spmi.2016.08.018.

19. M. Batı, "Resonant Tunneling Properties of Laser Dressed Hyperbolic Pöschl-Teller Double Barrier Potential," *Physica E: Low-dimensional Systems and Nanostructures* 165 (2024): 116126, https://doi.org/10.1016/j.physe.2024.116126.

20. A. K. Ghosh, Q. Marsal, and A. M. Black-Schaffer, "Laser-Induced Topological Phases in Monolayer Amorphous Carbon," *Physical Review B* 113 (2026): L121402, https://doi.org/10.1103/tp7r-31dj.

21. D. Cimbri, B. Yavas-Aydin, F. Hartmann, et al., "Accurate Quantum Transport Modeling of High-Speed $In_{0.53}Ga_{0.47}As$/AlAs Double-Barrier Resonant Tunneling Diodes," *IEEE Transactions on Electron Devices* 69, no. 8 (2022): 4638–4645, https://doi.org/10.1109/ted.2022.3178360.

22. J. A. Gil-Corrales, J. A. Vinasco, M. E. Mora-Ramos, A. L. Morales, and C. A. Duque, "Study of Electronic and Transport Properties in Double-Barrier Resonant Tunneling Systems," *Nanomaterials* 12, no. 10 (2022): 1714, https://doi.org/10.3390/nano12101714.

23. J. Zhu, J. Cao, C. Song, B. Li, and Z. Han, "Numerical Investigation on the Convergence of Self-Consistent Schrödinger-Poisson Equations in Semiconductor Device Transport Simulation," *Nanotechnology* 35, no. 31 (2024): 315001, https://doi.org/10.1088/1361-6528/ad4558.

24. P. Chakraborty, S. Joshi, and M. Gambhir, "Theoretical Analysis of Laser-Assisted Intersubband Transitions in A Quantum Well with a Razavy Confining Potential Influenced by a Static Electric Field," *Indian Journal of Physics* 100 (2025): 759–768, https://doi.org/10.1007/s12648-025-03779-7.

25. O. Ozturk, B. O. Alaydin, D. Altun, and E. Ozturk, "Intense Laser Field Effect on the Nonlinear Optical Properties of Triple Quantum Wells Consisting of Parabolic and Inverse-Parabolic Quantum Wells," *Laser Physics* 32, no. 3 (2022): 035404, https://doi.org/10.1088/1555-6611/ac5516.

26. B. Alaydin, D. Altun, O. Ozturk, and E. Ozturk, "High Harmonic Generations Triggered by the Intense Laser Field in GaAs/$Al_xGa_{1-x}As$ Honeycomb Quantum Well Wires," *Materials Today Physics* 38 (2023): 101232, https://doi.org/10.1016/j.mtphys.2023.101232.

27. E. Kasapoglu, M. B. Yücel, and C. A. Duque, "Parabolic–Gaussian Double Quantum Wells Under a Nonresonant Intense Laser Field," *Nanomaterials* 13, no. 8 (2023): 1360, https://doi.org/10.3390/nano13081360.

28. K. A. Rodríguez-Magdaleno, F. M. Nava-Maldonado, E. Kasapoglu, M. E. Mora-Ramos, F. Ungan, and J. C. Martínez-Orozco, "Nonlinear Absorption Coefficient and Relative Refractive Index Change for Konwent Potential Quantum Well as a Function of Intense Laser Field Effect," *Physica E: Low-dimensional Systems and Nanostructures* 148 (2023): 115618, https://doi.org/10.1016/j.physe.2022.115618.

29. C. A. Dagua-Conda, J. A. Gil-Corrales, M. E. Mora-Ramos, A. L. Morales, and C. A. Duque, "Electronic Transport Properties in a One-Dimensional sequence of Laser-Dressed modified Pöschl-Teller Potentials," *Nanomaterials* 15, no. 13 (2025): 1009, https://doi.org/10.3390/nano15131009.

30. A. F. J. Levi, *Applied Quantum Mechanics* (Cambridge University Press, 2023), https://doi.org/10.1017/9781009308083.

27511200, 2026, 8, Downloaded from https://advanced.onlinelibrary.wiley.com/doi/10.1002/apxr.70152 by Recep Tayyip Erdoan Üniversitesi, Wiley Online Library on [24/11/2026]. See the Terms and Conditions (https://onlinelibrary.wiley.com/terms-and-conditions) on Wiley Online Library for rules of use; OA articles are governed by the applicable Creative Commons License